Arch. Metall. Mater. **63** (2018), 2, 575-579

DOI: 10.24425/118976

M. FATIH KILICASLAN*#, E. KARAKOSE**

EFFECT OF Sc ADDITION ON THE MICROSTRUCTURE AND MECHANICAL PROPERTIES OF MELT-SPUN Al-10Ni ALLOYS

In the present work, rapidly solidified Al-10Ni-XSc (X = 0, 1 and 2) alloys were fabricated by melt spinning under Ar atmosphere. The Effects of Sc on the microstructural and thermal properties and microhardness values were investigated by scanning electron microscopy (SEM), X-ray diffractometer (XRD) and a Vickers microhardness tester. Experimental results revealed that the addition of 2 wt. % Sc to melt-spun Al-10Ni alloys changed their brittle nature and hindered formation of cracks. The addition of Sc to melt-spun Al-10Ni alloys also changed the morphology of Al_3Ni intermetallics from an acicular/needle – like to a rounded particle-like structure and led to reduction in their size. Formation of the metastable Al_9Ni_2 phase was observed due to the higher constitutional undercooling caused by Sc addition. A considerable improvement in microhardness value (from 95. 9 to 230. 1 HV) was observed with the addition of Sc.

Keywords: Al-Ni-Sc alloys; Microstructure; Melt spinning; Microhardness

1. Introduction

Due to the rapid extraction of thermal energy from the liquid state to the solid state in melt spinning process, it is possible to achieve a decrease in particle sizes, extended solid solubility of alloying materials, and metastable partly amorphous or amorphous phases in alloy systems by cooling exceeding 10^7 Ks^{-1} [1, 2]. Among rapid solidification methods, melt spinning (MS) is the most effective method that can drastically improve mechanical properties and change the morphology of secondary phases in the Al alloys [2]. Among the different Al based alloys, the Al-Ni alloys have good high temperature properties. Because of high temperature properties of melt spun Al-Ni alloys are as good as those of ceramics and super alloys, they have attracted much attention for aerospace and automotive applications [3,4]. When the rapidly solidified Al-Ni alloy is used as engine parts, it is possible to reduce the engine weight around 12-25% by comparison with the current conventional engines [5]. In addition, Al-Ni RS alloys are used for radiant burner parts and furnace rolls for corrosion-resistant parts in the chemical industry. However, Al-Ni alloys often contain intermetallic phases such as Al_3Ni [6,7], which are beneficial for high temperature applications because of their characteristics such as high creep strength, high melting temperature, high corrosion and oxidant resistance, and low density. However, they are harmful for mechanical properties due to their brittle nature. That is why, brittle fracture, processing problems, and low ductility are the main disadvantages of Al-Ni alloys [8]. Therefore, to obtain improved morphological and mechanical properties, there has been a lot of work on Al-Ni alloys in the literature [6-9]. The morphological and mechanical properties of RS Al-Ni alloys can be improved by transition metals such as Mn, Fe, Cu, Mg etc. [3-4,6-7,9]. These transition metals cause fine dispersions of the second phase in the alloy matrix and so, it is possible to obtain high strength, thermal and corrosion resistance. According to the best of our knowledge, there is no detailed study on Al–10Ni alloys which has been added Sc in the open literature. Therefore, in our work, we have investigated the effect of Sc addition on the thermal, microstructural, and mechanical properties of MS Al-10Ni-xSc (x = 0, 1 and 2 wt.%) alloys.

2. Experimental

In this study, elemental Al (99.9% purity, Alfa Aesar catalog no: 10093), Ni (99.99% purity, Alfa Aesar catalog no: 35482), and Sc (99.9% purity, Alfa Aesar catalog no: 39996) were used to prepare the alloys of nominal composition Al-10Ni Al-10Ni-1Sc and Al-10Ni-2Sc. In the present study, all percentages are wt.% unless otherwise stated. The master alloys were first produced in an induction heating smelter. Melt-spun counterparts of the master alloys were produced using an EZE Nanotechnoloji EE01 melt-spinner, in which the molten alloy

* KASTAMONU UNIVERSITY, FACULTY OF ENGINEERING, DEPARTMENT OF MATERIALS SCIENCE AND NANOTECHNOLOGY ENGINEERING, 37150 KASTAMONU, TURKEY
** ERCIYES UNIVERSITY, KAYSERI VOCATIONAL SCHOOL, DEPARTMENT OF AUTOMOTIVE TECHNOLOGY, 38039 KAYSERI, TURKEY
# Corresponding author: fatihkilicaslan@yahoo.com

in a quartz crucible was ejected onto a polished copper wheel (20 cm diameter) with 20 m/s disc velocity by pressurized argon at a rate of 200 mbars. The resulting MS samples were 18-90 μm thick and 1-4 mm wide. All experimental processes were performed in Ar atmosphere. The melt-spun alloys were denoted as MS0, MS1 and MS2, and the numbers 0, 1 and 2 following MS denote the amount of wt.% Sc in the Al-10Ni alloys. All alloys used in the present work are given Table 1. The phase constituents of the samples were initially identified by X-ray diffraction (XRD) and the microstructural features including compositions were examined by scanning electron microscopy (SEM) with used secondary electron (SE) mode and the Atlas software was used in image processing of SEM images. Microhardness analyses were performed with a Vickers microhardness tester. It was ensured that for each hardness result, applied load of 50, 100 and 200 mN at least 10 measurements were made and then averaged.

TABLE 1

Chemical compositions of the melt-spun alloys

Sample	Ni (wt.%)	Sc (wt.%)	Al (wt.%)
MS0	10	0	bal.
MS1	10	1	bal.
MS2	10	2	bal.

3. Results and discussion

The scanning electron microscopy (SEM) micrographs from melt – spun Al-10Ni (MS0), Al-10Ni-1Sc (MS1) and Al-10Ni-2Sc (MS2) alloys are shown in Fig. 1. As seen, ribbons from MS0 (Fig. 1a) and MS1 (Fig. 1b) have cracks, but those from MS2 do not have any crack (Fig. 1c). The ribbons of MS0 and MS1 alloys (especially MS1) were so brittle that it was very difficult to hold and mold them for the metallographic procedures. Therefore, we can say that the addition of 2 wt. % Sc to melt-spun Al-10Ni alloys has changed their brittle nature and hindered the formation of cracks.

In Fig. 2 the SEM micrographs with higher magnification of the deeply etched MS0 (Fig. 2a), MS1 (Fig. 2b) and MS2 (Fig. 2c) alloys are given. According to these micrographs, the microstructure of the melt-spun Al-10Ni alloy consists of an aluminum matrix and acicular intermetallics with sizes changing from 1 mm to 5 mm (Fig. 2a). The addition of 1 wt. percent Sc brought about dramatic changes in the morphology and size of intermetallics, that is, their acicular-like morphology of them was converted to a rounded particle-like structure with sizes varying from 0.168 mm to 0.983 mm with the addition of 1 wt. % Sc (Fig. 2b). However, by increasing Sc addition to 2 wt. %, morphology of the intermetallics did not change so much, and their size changed from 0.20 mm to 1.55 mm. As far as the Al-Ni phase

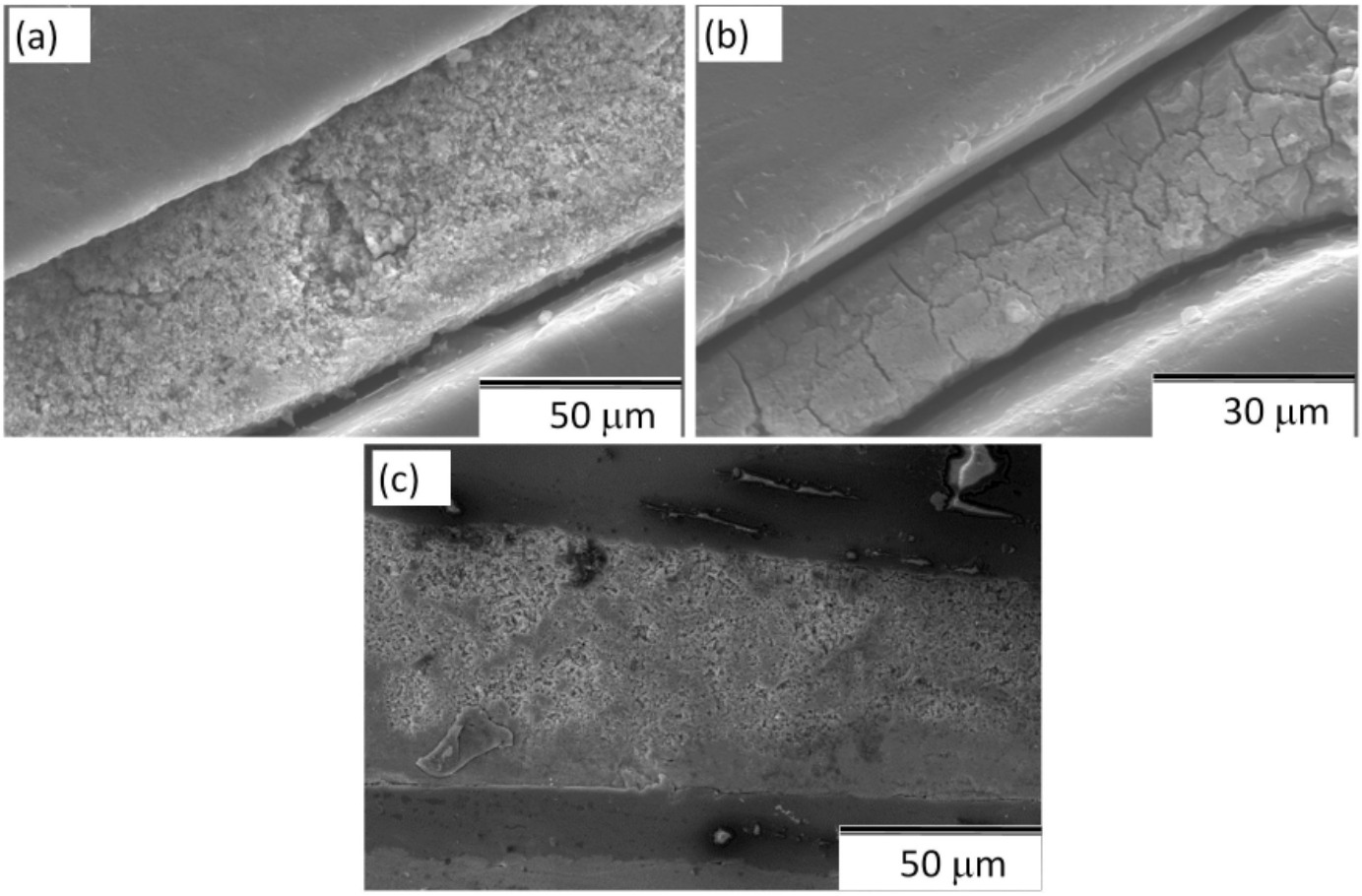

Fig. 1. Lower magnification SEM micrographs illustrating cross-sections of melt-spun Al-10Ni alloys with different amount Sc content; (a) base alloy (MS0), (b) 1 wt% Sc added alloy (MS1), (c) 2 wt% Sc added alloy (MS2)

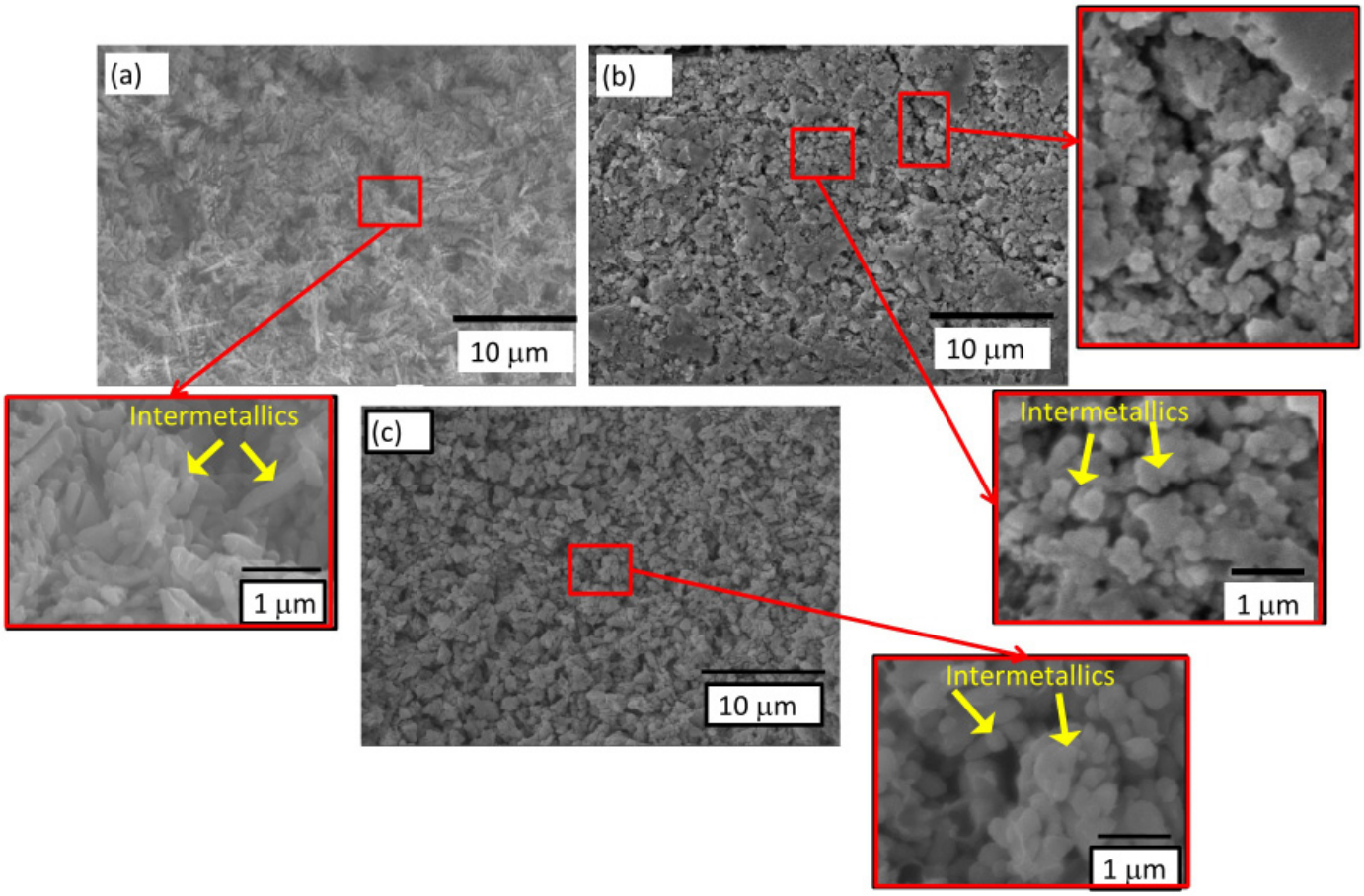

Fig. 2. SEM micrographs illustrating changes in the microstructure of melt-spun Al-10Ni alloys with different amount Sc addition; (a) base alloy (MS0), (b) 1 wt% Sc added alloy (MS1), (c) 2 wt% Sc added alloy (MS2)

diagram is concerned for a nominal composition of Al-10Ni, it can be anticipated to form Al_3Ni intermetallics embedded in the Al matrix. Al_3Ni needle intermetallics are responsible for the brittle nature of Al-Ni alloys [10].

According to the X-Ray diffractometer (XRD) analyses (Fig. 3), the microstructure of Sc free alloy MS0 contains Al_3Ni intermetallics and an Al matrix. Therefore, we think that the needle – like intermetallics seen in the microstructure of the SEM micrograph of the sample MS0 (Fig. 2a) is Al_3Ni. On the other hand, as is expected from the Al-Ni and Al-Ni-Sc phase diagrams [11], the microstructures of the alloys containing Sc MS1 and MS2 consist of Al_3Ni, Al_3Sc, Al_9Ni_2 and Al matrix, which is agreement with ref. [12]. This means that addition of Sc brought about formation of two additional intermetallic phases, that is, Al_3Sc and Al_9Ni_2. According to the Al-Sc phase diagram for an Al alloy containing 1 and 2 wt. percent Sc, the formation of Al_3Sc intermetallic phase can be expected [13]. However, the formation of the Al_9Ni_2 phase under the equilibrium condition is not normal. Gonzalez et al. [10] reported that, when they rapidly solidified Al – 4 at. % Ni alloy by melt spinning, they observed the formation of the Al_9Ni_2 phase, which is the richest intermetallic in terms of Al among all the metastable phases within the Al-Ni system. It is well known the literature that during melt spinning, an increased undercooling level is obtained because of very high cooling rate [14,15]. It is also reported in the literature that when Sc is added to Al alloys, an increased Sc concentration in the liquid phase leads to bigger constitutional undercooling [16,17]. Therefore, in our situation we can say that the formation of the metastable Al_9Ni_2 phase was due to higher constitutional undercooling caused by Sc addition.

Fig. 4 shows the DSC trace obtained during heating of the MS1 samples. Three similar endotherms appeared in the DSC trace of the MS alloy (Fig. 4). These endotherms had onset temperatures of 569, 625 and 641°C. Zhang and Du [18] reported that one of three invariant equilibria in the Al-rich region of the Al-Fe-Ni system is $L \Leftrightarrow (Al) + Al_9FeNi + Al_3Ni$ at 639 ± 2°C. In the Al alloys containing transition metal, there are intermetallic phases belonging to a monoclinic crystal structure and stoichiometric composition of Al_9X_2, that is Al_9Co_2 Al_9Fe_2 Al_9Ni_2 Al_9FeNi [19]. Therefore, we think that the peak seen at 641 °C (Fig. 4) could be related to the invariant transition equilibrium $L \Leftrightarrow (Al) + Al_9Ni + Al_3Ni$. On the other hand, Zhang et. al [18] stated that for Al-Sc-Si ternary alloys, the transition reaction is $L + Al_3Sc \Leftrightarrow (Al) + \tau\ (AlSc_2Si_2)$ + at 624°C. Nandi et al. [12] also reported that Sc can dissolve in binary Al-Ni intermetallics such as Al_3Ni and NiAl (Sc can substitute for both Ni and Al), resulting in Al-Ni-Sc ternary intermetallics such as $AlNi_2Sc$. Therefore, for the present study, the peak seen at 625°C (Fig. 4) should correspond to $L + Al_3Sc \Leftrightarrow (Al) + \tau\ (AlSc_yNi_x)$. That is, according to literature and DCS analyses, Al-Ni intermetallic

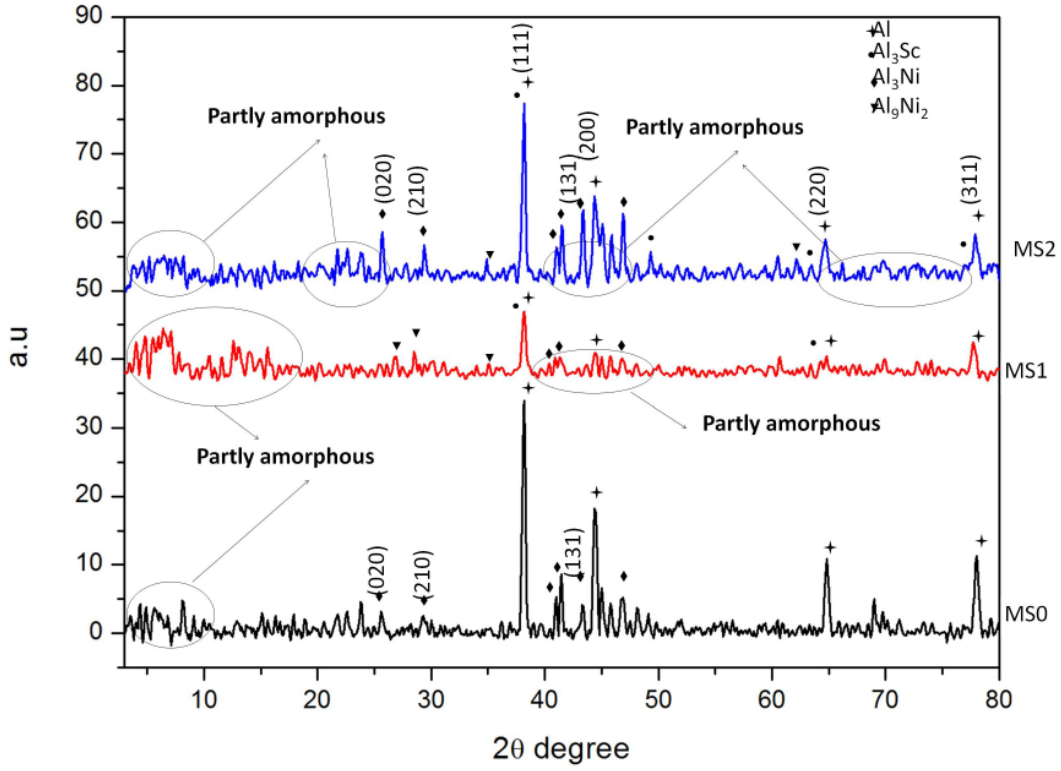

Fig. 3. XRD patterns of melt-spun Al-10Ni alloys with different amount Sc content

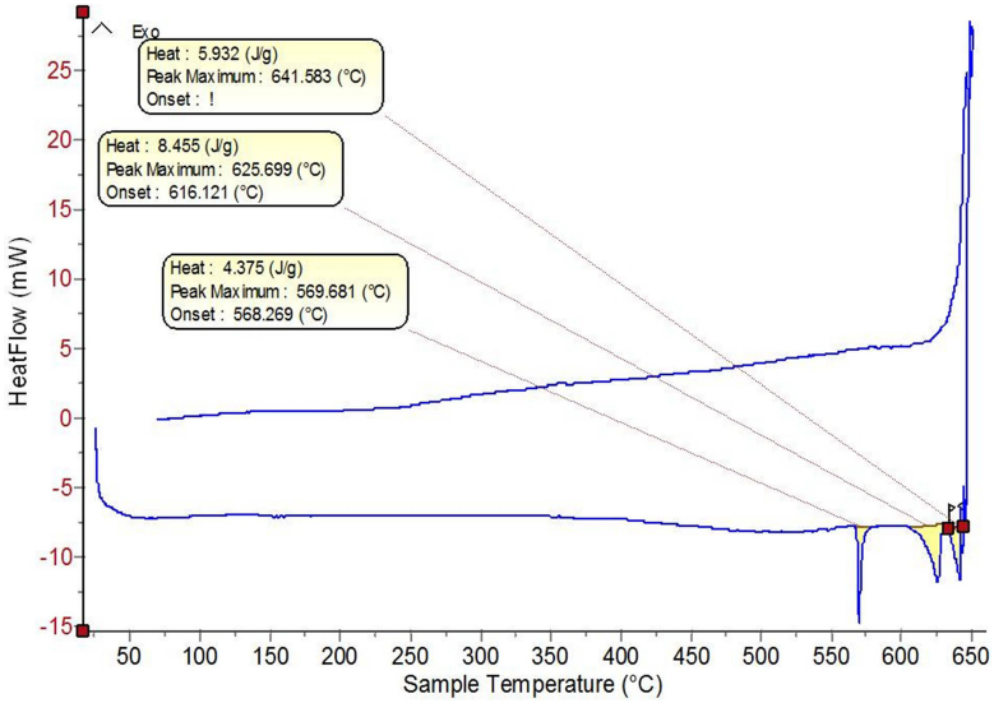

Fig. 4. DSC trace obtained from the Al-10Ni alloy with 1 wt. % Sc addition (MS1)

phases may also contain Sc. Therefore, the intermetallic phases of Al_3Ni and Al_9Ni_2 detected by XRD (Fig. 3) in the MS1 and MS2 samples can be Al_3NiSc and Al_9NiSc. As for the third peak seen at 569°C, we think that this can be attributed to the solid-state inter-diffusion that occurs between Al and Ni at the temperatures below the eutectic temperature, because, Morsi noted [20] that the solid-state inter-diffusion reactions related to the formation of Al-rich compounds such as Al_3Ni and Al_3Ni_2 can occur at temperatures considerably lower than that of the eutectic temperature (640°C), e.g. 550°C.

Fig. 5 illustrates changes in the microhardness values of all the melt-spun Al-10Ni alloys with addition of Sc. All microhardness values are an average value of 10 measurements for each specimen. It is clearly seen from Fig. 5 that, Sc addition to Al-

10Ni alloys caused considerable increments in the microhardness values. In particular in the alloy with Sc addition of 2 wt. %, there was a very dramatic increment in the microhardness value caused by Sc addition. The microhardness value of the MS0, MS1 and MS2 samples were 95.9, 112.2, and 230.1 HV, respectively. It has been reported in the literature that the modification and refining of coarse acicular secondary phases such as the coarse primary Si and Fe-bearing intermetallics seen in Al-Si alloy, reduce the probability of crack formation and improve the mechanical properties [21,22]. Therefore, one possible reason for the increment in the microhardness values could be particle size strengthening because the addition of Sc led to the refining and modification of needle-like coarse Al_3Ni intermetallics. On the other hand, it has also been reported that Sc brings about the highest increment of strengthening per atom percent when added to aluminum, increasing strength both by solid solution and precipitation hardening of the Al_3Sc particles [17]. Thus, considering that the maximum solid solubility of Sc in Al is 0.35 wt. percent and our alloys contain 1 and 2 wt. percent Sc, we think that the increment in the microhardness values may be attributed to the particle size strengthening as well as solid solution and precipitation hardening.

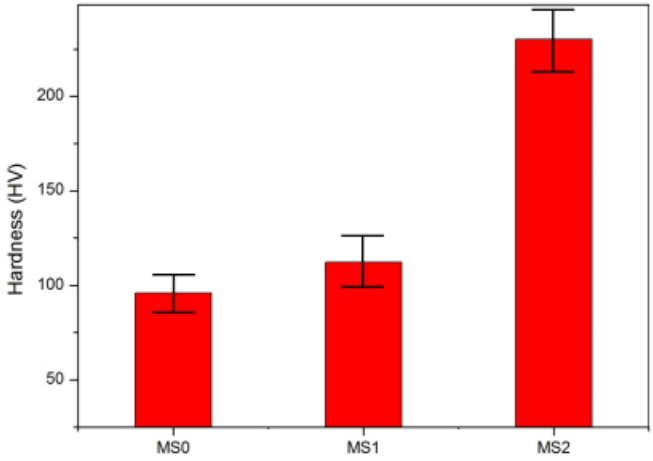

Fig. 5. Changes in microhardness values by Sc addition in MS0, MS1, and MS2 alloys

4. Conclusion

In summary, the present study reports the microstructure evolution and microhardness values of melt-spun Al-10Ni alloys with the addition of different amounts of Sc. The conclusions are as follows:

- It was observed that the addition of 2 wt. % Sc to melt-spun Al-10Ni alloys changed their brittle nature and hindered the formation of cracks.
- The addition of 1 and 2 wt. percent Sc to melt-spun Al-10Ni alloys changed the morphology of Al_3Ni intermetallics from acicular/needle – like to a rounded particle-like structure and led to a reduction in their size The formation of the metastable Al_9Ni_2 phase was observed due to higher constitutional undercooling caused by Sc addition.
- A considerable improvement in microhardness value (from 95.9 to 230.1 HV) was observed with the addition of Sc

REFERENCES

[1] E.J. Lavernia, T.S. Srivatsan, J. Mater. Sci. **45** (2), 287-325 (2010).
[2] H. Jones, Mater. Sci. Eng. A **304-306**, 11-19 (2004).
[3] T.S. Kim, S.J. Hong, B.T. Lee, Mater. Sci. Eng. A **363**, 81-85 (2003).
[4] H. Sieber, J.S. Park, J. Weıssmüller, J.H. Perepezko, Acta Mater. **49**, 1139-1151 (2001).
[5] E.F. Matthys, W.G. Truckner (Ed.), Melt spinning, Strip Casting and Slab Casting, TMS, Warrendale, 1996.
[6] M.T. Clavaguera-Mora, J. Rodriguez-Viejo, D. Jacovkis, J.L. Touron, N. Clavaguera, W.S. Howells, J. Non-Cryst. Solids **287**, 162-166 (2001).
[7] F. Audebert, C. Mendive, A. Vidal, Mater. Sci. Eng. A **375-377**, 1196-1200 (2004).
[8] N.S. Stoloff, C.T. Liu, S.C. Deevi. Intermetallics **9-11**, 1313-1320 (2008).
[9] S.H. Wang, X.F. Bian, J Alloy Compd. **453**, 127-139 (2008).
[10] G. Gonzalez, G.A. Rodriguez, S. A. Jimenez., W. Saikaly, A. Charai, Mater. Charact. **59**, 1607-1612 (2008).
[11] H. Okamoto, Phase diagrams for binary alloys. Materials Park (USA): ASM International **426**, 311 (2000).
[12] P. Nandi, S. Suwas, S. Kumar, K. Chattopadhyay, Metall. Mater. Trans. A **44**A, 2591-2603 (2013).
[13] Y. Castrillejo, A. Vega, M. Vega, P. Hernández, J.A. Rodriguez, E. Barrado, Electrochem. Acta **118**, **58**-66 (2014).
[14] M.F. Kilicaslan, F. Yilmaz, S.J Hong, O. Uzun, Mater. Sci. Eng. A **556**, 716-721 (2012).
[15] M.F. Kilicaslan, F. Yilmaz, S. Ergen. S.J. Hong, O. Uzun, Mater. Charact. **77**, 15-22 (2013).
[16] W. Prukkanon, N. Srisukhumbowornchai, C. Limmaneevichitr, J. Alloy Compd. **477**, 454-460 (2009).
[17] W.G. Zhang, Y.C. Ye, L.J. He, P.J. Li, X. Feng, L.S. Novikov, Mater. Sci. Eng. A **578**, 35-45 (2013).
[18] L. Zhang, Y. Du, Comput. Coup. Phase. Diag. Thermochem. **31**, 529-540 (2007).
[19] A. Yamamoto, H. Tsubakino, Scripta Mater. **37**, 1721-1725 (1997).
[20] K. Morsi, Mater. Sci. and Eng. R **A299**, 1-15 (2009).
[21] S.J. Hong, C. Suryanarayana, Metall. Mater. Trans. A **36A**, 715-723 (2005).